

1 Trade off predictivity and explainability for ML-
2 powered predictive toxicology: an in-depth
3 investigation with Tox21 datasets

4
5 Leihong Wu¹, Ruili Huang², Igor V. Tetko,³ Zhonghua Xia,³ Joshua Xu¹, Weida Tong^{1*}

6 1 Division of Bioinformatics and Biostatistics, National Center for Toxicological Research, FDA. 3900
7 NCTR Rd., Jefferson, Arkansas, 72079, USA

8 2 Division of Preclinical Innovation, National Center for Advancing Translational Sciences, National
9 Institutes of Health, 9800 Medical Center Drive, Rockville, Maryland 20850, USA

10 3 Institute of Structural Biology, Helmholtz Zentrum München-Research Center for Environmental Health
11 (GmbH), Ingolstädter Landstraße 1, 85764, Neuherberg, Germany

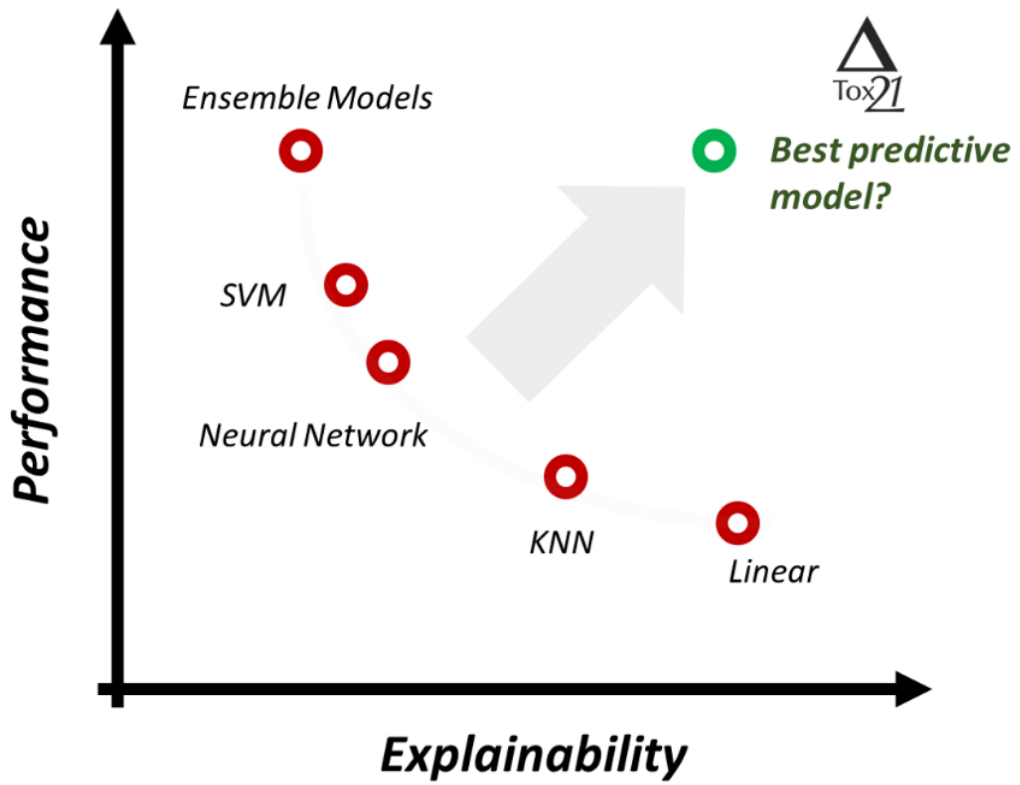
12
13

14 *Disclaimer: The views presented in this article do not necessarily reflect those of the U.S.*
15 *Food and Drug Administration or the National Institutes of Health. Any mention of*
16 *commercial products is for clarification and is not intended as an endorsement.*

17
18

19

20 For TOC only:
21



22
23

24 Abstract

25 Selecting a model in predictive toxicology often involves a trade-off between prediction
26 performance and explainability: should we sacrifice the model performance to gain
27 explainability, or vice versa? Here we present a comprehensive study to assess algorithm and
28 feature influences on model performance in chemical toxicity research. We conducted over
29 5000 models for a Tox21 bioassay dataset of 65 assays and ~7600 compounds. Seven
30 molecular representations as features and twelve modeling approaches varying in complexity
31 and explainability were employed to systematically investigate the impact of various factors
32 on model performance and explainability. We demonstrated that endpoints dictated a model's
33 performance, regardless of the chosen modeling approach and chemical features. Overall,
34 more complex models such as (LS-)SVM and Random Forest performed slightly better than
35 simpler models such as linear regression and KNN in the presented Tox21 data analysis.
36 However, when a simpler model yielded acceptable performance for the Tox21 dataset, it
37 clearly was the preferred choice due to its better explainability. Given that each dataset had
38 its own error structure both for dependent and independent variables, we strongly recommend
39 that it is important to conduct a systematic study with a broad range of model complexity and
40 feature explainability to identify model balancing its predictivity and explainability.

41

42 Keywords

43 Tox21 bioassay, QSAR model, machine learning, predictive toxicology, explainable artificial
44 intelligence (AI), explainability, interpretability.

45

46 Background

47 Artificial Intelligence (AI) has been playing an increasingly vital role in a broad range of
48 scientific research and applications, including clinical diagnosis/prognosis, natural language
49 processing, speech and face recognition, and machine translation. Recent development of
50 neural networks, commonly known as Deep Learning (DL), have further speeded up
51 development of AI by taking advantage of Big Data and increased computational power.
52 Highlighted as one trigger event in 2012, the award-winning DL model (AlexNet) held a top-
53 5 error rate of 15.3% in the ImageNet Large Scale Visual Recognition Challenge (ILSVRC),
54 demonstrating a significant improvement over the second-best model's top-5 error rate of
55 26.2%¹. Since then, complex modeling algorithms such as DL have gained wide acceptance,
56 leading to better model performance, especially in Big Data analysis.

57 In predictive toxicology, AI and Machine Learning (ML) also has been widely investigated
58 for chemical risk assessment and drug safety evaluation. In the past decades, our group
59 developed numerous predictive toxicology approaches and tools in this area, particularly for
60 drug-induced liver injury (DILI)²⁻⁶ and toxicogenomics⁷⁻⁹. The combination of high
61 throughput screening and ML has also become an important direction in predictive
62 toxicology¹⁰⁻¹². For instance, the Tox21 project has screened over 10000 chemical
63 compounds via robotic automated high-throughput in vitro assays to measure corresponding
64 bioactivities, an unprecedented achievement which provided millions of chemical bioactivity
65 profiles and data points.^{10, 13}

66 One of the key ML applications in predictive toxicology is to predict chemical bioactivities,
67 including toxicity with molecule structure. Traditionally known as QSARs (quantitative
68 structure activity relationships), this field has seen significant advancements with modern
69 machine learning approaches, such as Support Vector Machine (SVM), Random Forest, and
70 recently DL^{9, 14, 15}. For instance, several DL approaches have been developed recently with
71 QSAR studies¹⁶⁻¹⁹, most of which reported improved prediction accuracy for different tasks.
72 Along with improved performance, another advantage of some DL approaches is their innate
73 ability to work with molecular representation as SMILES, chemical graphs or images and
74 thus bypassing the manual feature selection process.^{20, 21} While on one side this may remove
75 a bias of a researcher to one or another type of descriptors it may also result in DL models

76 which are more opaque since the reasoning for the model decisions is buried amid millions of
77 neural network weights.

78 The problem of model interpretations is actively pursued in chemoinformatics²² where it is
79 going beyond the traditional QSAR and is highly relevant in other fields of science²³. A
80 prerequisite for a trustworthy model is that its performance can be explained. Explainability
81 can be defined as an AI behavior that can be understood and accepted by human, which
82 involves many concepts and aspects such as transparency, interpretability, causality,
83 transferability, accessibility, etc.²⁴ This is a topic of active research in explainable Artificial
84 Intelligence and some promising development in this area were recently reported elsewhere²³,
85 ²⁵. Still some methods, such as a linear regression, k-nearest neighbors (kNN) or decision
86 trees, which are used by researchers since many years, are considered as more interpretable
87 since, e.g., the weight of features in regression could be interpreted as its importance to the
88 decision making. In predictive toxicology, the driving features are descriptors of a
89 substance's biological and chemical properties. Since human experts could explain influence
90 of physiochemical descriptors, a predictive model developed with them generally could be
91 more easily interpretable than the one using more complex features such as hashed
92 fingerprints, graphical/geometric depictions and/or ML-derived molecular representations.
93 With that said, the selection of chemical features and the complexity of modeling algorithm
94 are currently the key factors to determine the explainability in predictive toxicological
95 research.

96 The choice of modeling algorithm frequently involves a perceived trade-off between
97 predictivity and explainability. In other words, increasing predictivity sometimes could lead
98 to lower explainability; the reverse also could be true. The challenge is how we can balance
99 predictivity and explainability to achieve a trustworthy model. To achieve that, we first need
100 to understand how much the selection of model algorithms, as well as chemical features,
101 would impact predictivity. In this study, we report a case study using the Tox21 bioassay
102 activity dataset.^{26, 27} We mostly focus on the transparency and interpretability versus
103 prediction performance of analyzed methods for Tox21 endpoints, which is attributed to the
104 types of the modeling algorithms and the descriptors. We provide a broad view of ML
105 applications in predictive toxicology by systematically investigating the influence of assay
106 endpoints, modeling algorithms, and features and data processing procedures.

107 Methods and Materials

108 Tox21 Dataset

109 Tox21 bioassay activity data (the Tox21 Dataset¹³) were collected for 68 bioassay
110 endpoints²⁷ and 8948 compounds, of which each was tested in at least one assay. Chemical
111 bioactivity data was preprocessed and categorized into four major classes: active agonist,
112 active antagonist, inactive and inconclusive²⁸. In this study, both active agonists and active
113 antagonists were considered positive compounds, and inactives were considered negative.
114 Only one active category was considered in each assay; i.e., if one assay contained more
115 active agonists than active antagonists, we used the active agonists as positive in the analysis.
116 Inconclusive compounds were excluded from all assays/endpoints. Chemicals were further
117 deduplicated based on their InChI keys. The final number of positive and negative samples in
118 each assay was summarized in **Supplementary Table S1** and all processed data are available
119 as **Supplementary Table S2**.

120 In addition, the chemical similarity of a Tox21 assay endpoint was calculated using a within-
121 group chemical similarity (S) score. S represented the chemical diversity in accordance with
122 the endpoint, which was measured according to formula (1). In the formula, m and n
123 represent the number of compounds in positive and negative classes, respectively. $Jaccard_{ij}$
124 indicates the Jaccard similarity coefficient (index) between compounds i and j , which was
125 calculated based on RDkit fingerprints. As formulated, higher S value corresponds to
126 endpoint with compounds that are more similar within the class of actives.

$$S = Mean(\sum_{i=1}^m \sum_{j=1}^m Jaccard_{ij}) - Mean(\sum_{i=1}^m \sum_{k=1}^n Jaccard_{ik}) \quad (1)$$

127

128 Predictive modeling algorithms

129 In total, 12 modeling algorithms were included in this study; These modeling algorithms can
130 be categorized into four classes: (1) neural networks; (2) decision trees ensemble methods; (3)
131 SVMs; and (4) simple algorithms. For neural networks, we deployed a 3-Layer neural-
132 network(MLP-3), 7-Layer neural-network (DNN¹⁹), Associative Neural Network (ASNN-
133 MTL)²⁹, and a Multi-task Learning version of the 7-Layer Neural-network (DNN-MTL)¹⁹.
134 Algorithm ending with MTL were performed with multi-task learning framework. Four

135 decision trees ensemble methods, XGBoost³⁰, AdaBoost, GradientBoosting, and Random
 136 Forest, were used. For SVMs, we applied rbf SVM (SVM)^{31,32} and Least-Squares SVM (LS-
 137 SVM)³³ optimized for GPU-based computing. Lastly, Linear Regression and KNN were used
 138 as for simple algorithms³². These modeling algorithms provided broad coverage of modeling
 139 complexity while representing popular modeling algorithms in the field. Linear regression
 140 and KNN are simple methods that are easier to understand, while SVMs and neural networks
 141 are relatively more complicated and difficult to interpret. The use of ensembles for decision
 142 trees despite it added more complexity was also shown to significantly improve their
 143 performances^{30,34}. Deep neural-networks are one of the recent popular modeling algorithms
 144 and often have good predictivity compared to other algorithms especially in studies dealing
 145 with large data^{14,21,35}.

146 Among the 12 studied algorithms, XGBOOST, LS-SVM, DNN, ASNN-MTL and DNN-
 147 MTL were performed in OCHEM platform (<http://ochem.eu>), which has LS-SVM and
 148 DNN(-MTL) implemented using GPU.³⁶ The other seven modeling algorithms were
 149 performed on local computing cluster at FDA. As designed, the training and testing
 150 compounds for two experiment sites were exactly the same, but we applied slightly different
 151 data-preprocessing strategy on each site. For example, correlation filters (>0.95) was used in
 152 OCHEM platform for feature reduction during data pre-processing. We checked the influence
 153 of the preprocessing on the performance of the Random Forest, which was calculated with
 154 the same setting of hyperparameters in OCHEM and FDA sites but did not observe any
 155 systematic bias. The parameters used in these modeling algorithms, if not specified, were set
 156 to defaults, which were optimized in multiple studies performed by their authors. The details
 157 of modeling algorithms used in this study are summarized in **Table 1**.

158

159 **Table 1.** Brief summary of modeling algorithms used in this study.

SYNONYM	MODELING ALGORITHM	CATEGORY	PARAMETERS
LINEAR	Linear regression	Simple Model	
KNN	K-Nearest Neighbors	Simple Model	K=5 (default)
RF	Random Forest	Ensemble Model	n=100 (default)
ABOOST	Adaptive Boosting	Ensemble Model	n=50 (default)
GBOOST	Gradient Boosting	Ensemble Model	n=100 (default)

XGBOOST	Extreme Gradient Boosting	Ensemble Model	
SVM	Support Vector Machine	SVMs	Kernel=rbf; C=100; gamma='scale'
LS-SVM	Least-Squares SVM	SVMs	
MLP3	3 layers Multi-layer Perceptron	Neural Networks	nodes=[32, 64, 32];
DNN	7 layers Neuro Networks	Neural Networks	nodes=[512:256:128:64:32:16]
DNN-MTL	Multi-Task Learning of DNN	Neural Networks	Same as above
ASNN-MTL	Associative neural network	Neural Networks	Ensemble of 64 models with one hidden layer containing 3 neurons

160

161 Chemical Features

162 We evaluated seven different types of chemical features to represent the chemical structures,
 163 five chemical fingerprints (i.e., RDKit³⁷, ECFP4, FCFP4, Extended Functional Groups
 164 (EFG)³⁸ and ToxPrint³⁹) and two QSAR descriptors (i.e., MordRed⁴⁰ and Mold2⁴¹). RDKit
 165 fingerprint was developed by RDKit³⁷ and was calculated with default parameters
 166 (nbits=2048). Extended-Connectivity Fingerprints (ECFP4 and FCFP4) are atom-based and
 167 feature-based chemical fingerprints, both of which were calculated by using Morgan
 168 fingerprints generated by the RDKit, with radius=2 and bit length 1024. ToxPrints are based
 169 on the publicly available ToxPrint chemotypes (v2.0_r711, <https://toxprint.org/>) generated
 170 within the associated ChemoTyper application (<https://chemotyper.org/>). EFG is an extension
 171 of a functional group set previously implemented by the CheckMol⁴² that also covers
 172 heterocyclic compound classes and periodic table groups³⁸. ToxPrint chemotypes consist of
 173 729 uniquely defined chemical features coded in XML based Chemical Subgraphs and
 174 Reactions Markup Language (CSRML). The numbers of features generated for each type of
 175 descriptors are listed in **Table 2**.

176

177 **Table 2.** Brief summary of feature generation tools used in this study.

SYNONYM	#FEATURES	CATEGORY	REFERENCE
RDKIT	2048	Chemical fingerprints	https://www.rdkit.org
ECFP4	1024	Chemical fingerprints	https://www.rdkit.org
FCFP4	1024	Chemical fingerprints	https://www.rdkit.org
EFG	583	Chemical fingerprints	Citation ³⁸

TOXPRINT	729	Chemical fingerprints	https://toxprint.org , ³⁹
MORDRED	1825	QSAR descriptors	Citation ⁴⁰
MOLD2	777	QSAR descriptors	Citation ⁴¹

178

179 Results

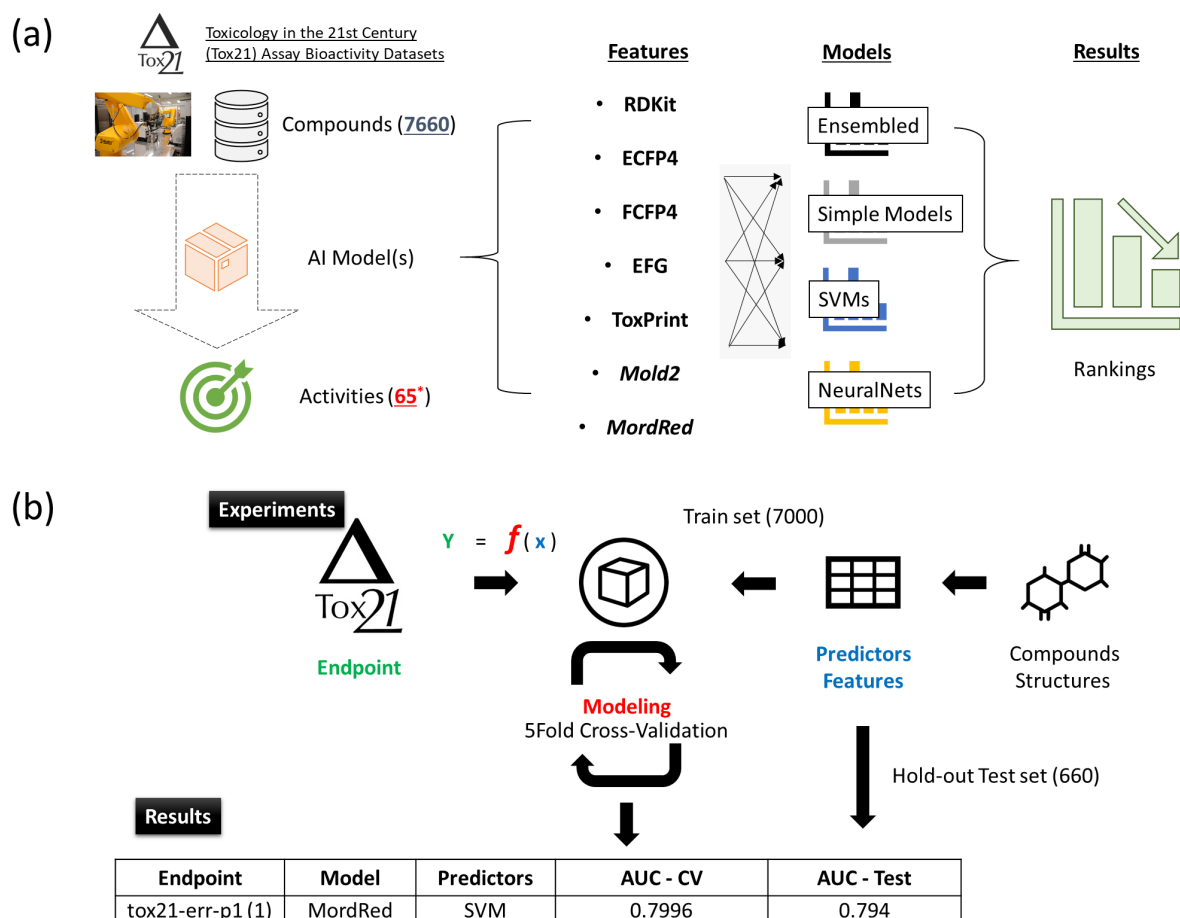
180 Study workflow

181 The overall study design is depicted in **Figure 1a**. We used all publicly available assays from
 182 the Tox21 dataset¹³ to take advantage of the diversity in assayed endpoints (i.e., 68
 183 bioactivity endpoints). In total, 8948 compounds were profiled by at least one assay. After
 184 data pre-processing to remove chemical duplicates, 7660 compounds were retained for the
 185 analyses. These compounds were split on training and test set comprising 7000 and 660
 186 compounds, respectively (see Supplementary Table S2). We conducted binary classification
 187 and for each assay only active and inactive compounds were considered. The active
 188 compounds could either be active agonists or active antagonists, depending on the majority
 189 group of the assay (see Materials and Methods for details). For duplicated compounds, only
 190 compound with consistent bioactivities in the same assay were considered: others were
 191 labeled as inconclusive and discarded. Finally, we removed three assays that did not have
 192 enough active compounds (≤ 20), therefore 65 Tox21 assays remained for modeling analysis.
 193 The final processed-ready dataset is available for download from <http://ochem.eu> and is also
 194 included as Supplementary Table S2.

195 For each endpoint, we developed 84 models with exhaustive combination of seven types of
 196 molecular features in conjunction with 12 modeling algorithms. Specifically, we used RDkit,
 197 ECFP4, FCFP4, EFG, ToxPrint, Mold2 and MordRed to measure/represent different types of
 198 compound fingerprints or QSAR descriptors. Four major categories of 12 modeling
 199 algorithms were used to represent the varying degrees of complexity in modeling algorithms.

200 **Figure 1b** shows the general modeling pipeline with a single experiment (i.e., one feature set
 201 and one modeling algorithm applied to data from a single assay), in which a model pairing a
 202 modeling method with chemical features was evaluated by 5-fold cross-validation. During
 203 the cross-validation, we split the training dataset into 5 folds, where 4 folds were used for
 204 training and the other fold was used for validation. Next, the models were tested on the hold-
 205 out samples from the test set, which contains 660 unseen compounds. Final model

206 performance thereafter was measured by the average AUC of the training set as well as the
 207 AUC of testing set.



208

209

210 **Figure 1.** The overview of the workflow used to analyze the data. (a) Overall study design. (b) Construct
 211 and evaluate predictive model with selected predictor, modeling algorithm and endpoint.

212

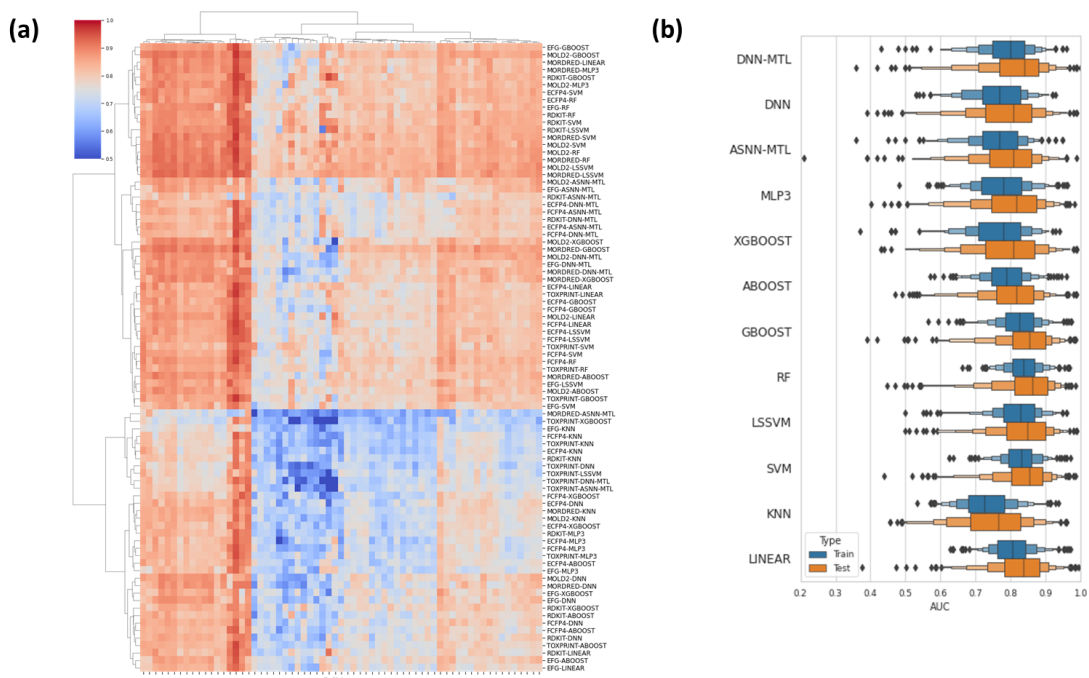
213 Model predictive performance

214 Overall results on the testing data are shown in **Figure 2a**. As shown, each cell in this
 215 hierarchical clustering map (HCA) is the average testing AUC from the nested cross
 216 validation results in one model. The x-axis contains 65 Tox21 assays. The HCA map contains
 217 84 rows, which represented all combinations of seven feature sets and 12 modeling
 218 algorithms.

219 First, we found that these 65 Tox21 assay endpoints showed very different performance
 220 patterns. Some endpoints always had a high AUC regardless of the type of feature or

221 modeling algorithm used. Contrary to that some endpoints showed a consistently low AUC
222 across all feature-algorithm combinations. With respect of their performance similarity
223 models using the same chemical features tended to cluster together.

224 The overall predicting performance for each Tox21 assay was summarized in the box-plot
225 representation (**Figure 2b**). Each bar represented a collapsed result of one particular
226 modeling algorithm, by combining all features and endpoints. Training (i.e., Cross-validation)
227 and testing (i.e., hold-out) results were presented in blue and orange boxes, respectively. As
228 shown, there was no significant performance gap between Training and Testing results,
229 indicating that the developed models were robust. Detailed model performances (AUC) for
230 each Tox21 assay were summarized in **Table S1**.



231

232 **Figure 2.** (a) Heatmap of all Tox21 assays across different modeling algorithms and features. (b)
233 Overall, collapsed performance for all Tox21 assays. The validation and testing results are consistent
234 across all endpoints;

235

236 Overall performance of model algorithms and features

237 Further analysis was applied to inspect the overall influence of chemical features and
238 modeling algorithms, by averaging the results across all 65 Tox21 endpoints. The 5-fold CV
239 and the hold-out testing results were summarized in **Table 3**.

240 Regarding to the feature types, the best feature type was Mold2 (AUC-CV=0.82; AUC-
241 test=0.84). The weakest feature type was ToxPrint (AUC-CV=0.76; AUC-test=0.78). In
242 general, QSAR descriptors (i.e., Mold2 and MordRed) performed better than chemical
243 fingerprints. We also observed that EFG outperformed ToxPrint, both of which were kinds of
244 structural alerts or functional groups.

245 On the other hand of modeling algorithms, we found GBoost, RF and SVMs showed better
246 predicting performance than other categories of algorithms, and the best modeling algorithms
247 among 12 we tested was RF (AUC-CV=0.84; AUC-test=0.84); the relatively weakest
248 modeling algorithm was KNN (AUC-CV=0.73; AUC-test=0.75). In addition, we did not
249 observe better performance of more complicated models such as the neural networks,
250 compared to simple models of Linear Regression, which provided similar results on average.
251 In addition, XGBOOST did not improve the model predictivity compared to GBoost. We also
252 observed that Multi-task learning framework may improve the modeling predictivity since
253 DNN-MTL outperformed DNN thus confirming results of other studies.

254 For the single pair of model-feature combination, LS-SVM with MordRed held the best
255 performance in average 65 Tox21 endpoints prediction (AUC-CV=0.87; AUC-test=0.88).
256 Note that the predictivity differences among top combinations were marginal; such as LS-
257 SVM-Mold2, LS-SVM-MordRed, RF-Mold2 and RF-MordRed, all of which held AUC
258 around 0.88 in hold-out testing result.

259

260

261 **Table 3.** Averaged performance of seven feature types and twelve modeling algorithms.

Model/ Feature	RDKit		ECFP4		FCFP4		EFG		TOXPRINT		MOLD2		MORDRED		Average	
	5-fold CV	Test	5-fold CV	Test	5-fold CV	Test	5-fold CV	Test	5-fold CV	Test	5-fold CV	Test	5-fold CV	Test	5-fold CV	Test
DNN-MTL	0.79	0.83	0.79	0.80	0.79	0.76	0.86	0.81	0.72	0.77	0.82	0.84	0.81	0.84	0.8	0.81
DNN	0.78	0.81	0.77	0.79	0.78	0.79	0.82	0.77	0.71	0.70	0.78	0.81	0.77	0.81	0.77	0.78
ASNN-MTL	0.77	0.76	0.80	0.84	0.79	0.84	0.84	0.81	0.73	0.79	0.80	0.81	0.66	0.67	0.77	0.79
MLP3	0.76	0.80	0.75	0.78	0.75	0.77	0.77	0.75	0.76	0.80	0.83	0.83	0.83	0.85	0.78	0.8
XGBOOST	0.79	0.81	0.76	0.77	0.75	0.77	0.80	0.78	0.67	0.69	0.81	0.85	0.81	0.85	0.77	0.79
GBOOST	0.83	0.85	0.81	0.83	0.80	0.81	0.83	0.83	0.81	0.83	0.85	0.87	0.84	0.87	0.83	0.84
ABOOST	0.77	0.79	0.76	0.78	0.77	0.78	0.80	0.79	0.78	0.81	0.82	0.83	0.89	0.84	0.79	0.8
RF	0.84	0.84	0.83	0.83	0.82	0.81	0.86	0.83	0.82	0.81	0.86	0.88	0.86	0.88	0.84*	0.84*
LS-SVM	0.84	0.86	0.82	0.83	0.81	0.84	0.84	0.82	0.73	0.74	0.86	0.88	0.87*	0.88*	0.83	0.83
SVM	0.84	0.85	0.83	0.84	0.81	0.82	0.81	0.80	0.81	0.81	0.85	0.87	0.85	0.88	0.83	0.84
KNN	0.73	0.77	0.73	0.74	0.72	0.73	0.71	0.70	0.72	0.75	0.76	0.79	0.77	0.80	0.73	0.75
Linear	0.79	0.81	0.81	0.82	0.81	0.82	0.81	0.78	0.81	0.83	0.82	0.83	0.82	0.85	0.81	0.82
Average	0.79	0.81	0.79	0.80	0.78	0.80	0.81	0.79	0.76	0.78	0.82*	0.84*	0.81	0.84		

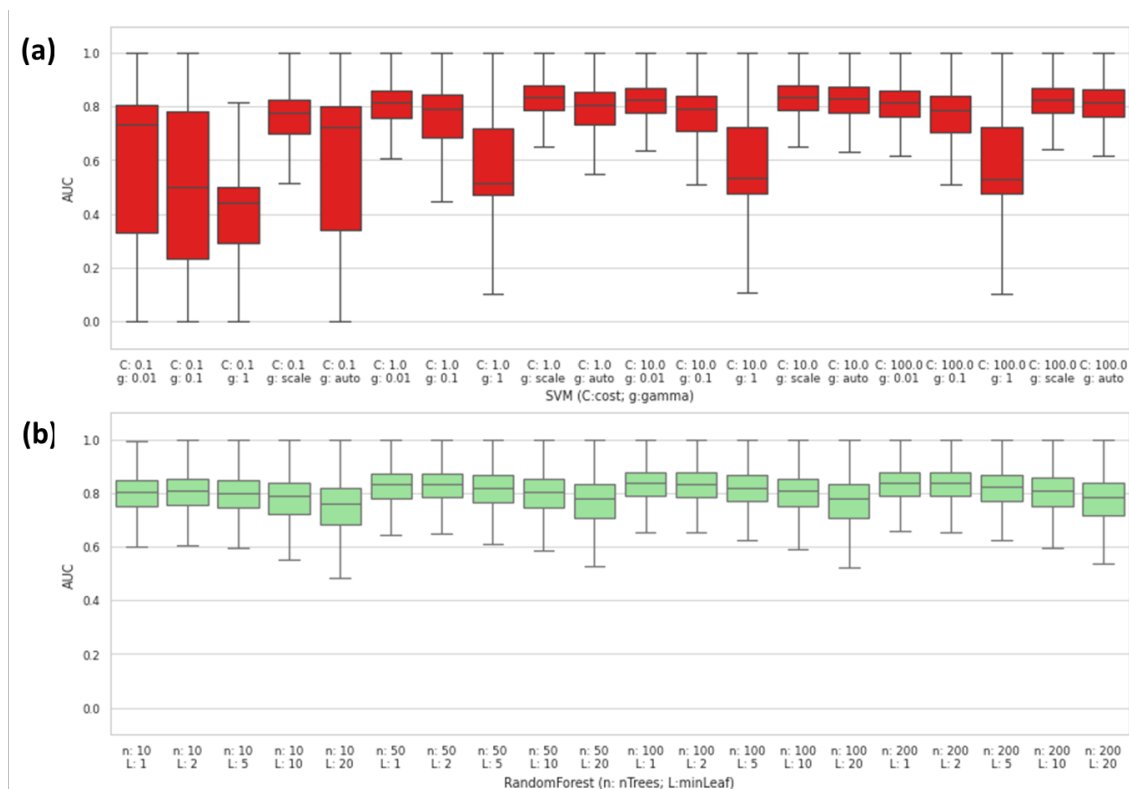
262 *Stars indicate the best performing descriptor sets and algorithms.

263 Parameter influence on predictivity of SVM and RF

264 Based on the overall prediction results, SVM and Random Forest (RF) showed a good
 265 predictivity among all feature types and endpoints we tested. Both RF and SVM have hyper-
 266 parameters, which may have significant impacts on the model performance. In aims to
 267 understand how much the hyper-parameter tuning could affect the predictivity of both SVM
 268 and RF, we performed a grid search analysis to fine-tune “cost parameter” (C) and gamma (g)
 269 for SVM (with default RBF kernel) and “number of trees” (n) and “minimal number of
 270 samples in leaf node” (L) for RF, respectively.

271 As shown in **Figure 3a**, the hyper-parameters showed a large impact on SVM models. As a
 272 “proper” set of hyper-parameters (e.g., C=10 and g = “scale”)⁴³ would achieve over 0.8 AUC
 273 across all types of features and endpoints where an “improper” set of hyper-parameters (e.g.,
 274 C=0.1 and g =1) would fail completely (Averaged AUC<0.5). On the other hand, we found
 275 that the influence of hyper-parameters on RF models was much smaller in comparison to
 276 SVM models (**Figure 3b**), as the “worst” set of hyper-parameters (e.g., n=10; L=20) still
 277 could get an averaged AUC around 0.75. Taken together, our findings demonstrated that

278 hyper-parameter selection can have a larger impact on some modeling algorithms such as
279 SVM, while less affects other modeling algorithms such as RF.



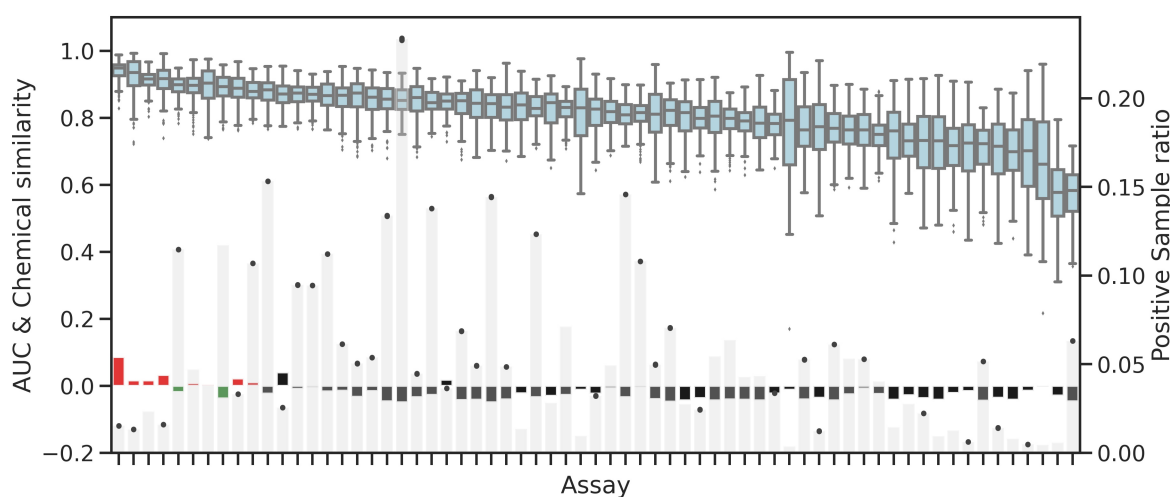
280

281 **Figure 3.** Hyper-Parameter tuning result for (a) SVM and (b) Random Forest.

282 Influence of sample size and chemical similarity on endpoint predictability

283 **Figure 4** shows an assessment of the other two important innate properties of a dataset that
284 affect model performance, sample size and chemical similarity. Due to data availability,
285 sample size varied from endpoint to endpoint, and the positive sample size (i.e., number of
286 active agonist or antagonist in the dataset) was usually much smaller than negative sample
287 size. A smaller positive sample leads to more imbalanced dataset, which could affect the
288 model performance. We therefore analyzed the correlation between model performance and
289 positive sample ratio for the analyzed endpoint (**Figure 4**, light gray bars). As shown, we
290 found that the positive sample size had little effect on the averaged model performance.
291 However the sample size influenced the variation of the performance and we observed wider
292 boxes and quantiles in assays with smaller positive sample sizes. In addition, lower
293 performed assays also tended to have larger variations of performance, which indicated the
294 modeling algorithm and feature selection could more affect these low-performed and less
295 sample size endpoints.

296 With respect to the chemical similarity of endpoints, the S scores were negative for most of
297 the Tox21 assays, indicating that for most assays, compounds within the respective
298 positive/active class shared low structural similarity (**Figure 4**, Red/Green/Black bars).
299 Meanwhile, we found that the S scores for eight of ten endpoints with high predictability
300 were positive, implying that higher structural similarity within the positive/active compound
301 class may contribute to the higher predictive performance of the models for these assays.
302 However, endpoints with negative S score did not necessarily result in poor performance; for
303 example, although assays of tox21-ahr-p1 and tox21-pr-bla-antagonist (green bars in Figure 4)
304 had negative S score -0.018 and -0.037 respectively, they still had high AUC (>0.85) in both
305 training and testing results.



306
307

308 **Figure 4.** Influences of positive sample ratio (light-gray bars) and sample within-group similarity
309 (green/red/black bars) on endpoint performance (blue box plot). Green and red bars are the top ten highest
310 performed assays with positive and negative S score, respectively,

311 Discussion

312 We conducted a systematic investigation on the choice of modeling approaches and chemical
313 features in predictive toxicology, with a specific focus on comparative analysis of model
314 performance and explainability and the trade-off between them. Results demonstrated that the
315 assay or endpoint itself was the largest determining factor for model performance; a good
316 performance was reached for a predictable endpoint (high predictability) regardless of the
317 choice of modeling algorithm or feature type used⁴⁴. As implied in Figure 4, assays with
318 lower performance tended to have larger variations. The influence of modeling algorithm and

319 features was more pronounced for such endpoints as well as for those with more imbalanced
320 dataset (i.e., smaller positive sample sizes). For such endpoints it could be important to
321 conduct a systematic analysis by using a broad range of approaches of various model
322 complexity and feature explainability. For the Tox21 datasets studied here, we found that
323 using simple modeling approaches such as Linear Regression in a number of cases provided
324 models with similar performance to those of more complex approaches, such as neural
325 networks. Such models could be more preferable in the context of the computational
326 toxicology due to better balancing of their predictivity and interpretability. Of course, the
327 reported in this study results could be influenced by type of the data and used descriptors, but
328 the use of simple baseline models should not be ignored.

329 Not all datasets have the same complexity, which further emphasizes the need for evaluating
330 a broad range of modeling approaches and molecular representations. Three innate data
331 properties are of special importance: endpoint predictability, data imbalance, and size. With
332 respect to endpoint predictability, we only examined the chemical structure similarity within
333 and across class labels without considering the quality of the endpoints measurements
334 themselves. The results implied that a high chemical structure-driven predictability likely
335 resulted in a good performance, but the reverse was not entirely apparent.

336 An algorithm with a simple architecture, such as linear regression may not be the most
337 powerful, but it will be easily explainable when using interpretable descriptors. Algorithms
338 with more complicated architectures, such as (LS-)SVM or (deep) neural networks, may have
339 better statistical performance but can be more difficult to interpret. In this study, we did
340 observe that some more complex modeling algorithms had overall better prediction accuracy
341 as compared to simple algorithms such as linear regression and KNN. However, the influence
342 of a modeling algorithm was not as significant as the nature of the endpoint itself and in a
343 number of cases simpler and easier to interpret models with similar performances were
344 obtained. Selecting a complex but less explainable model could hinder its use due to possible
345 concerns with interpretation of its predictions for new data.

346 Therefore, when considering both predictivity and explainability in the context of chemical
347 feature based Tox21 data analysis, we recommend do not overlook using simple models: they
348 provide higher explainability while still can have similar performance as some more
349 complicated approaches. Another strategy is to increase the explainability of complex models
350 via model-agnostic approaches⁴⁵. With more such approaches being developed⁴⁶⁻⁴⁸ and with

351 their wider availability, complex models such as DL networks may hold great potential for
352 improved explainability. In their absence an interpreting a complex model is much more
353 difficult than interpreting a simple model such as linear regression. Given that each dataset
354 has its own error structure both for dependent and independent variables, we strongly
355 recommend that it is important to conduct a systematic study with a broad range of method
356 complexity and feature explainability to select a model, which balance its predictivity and
357 explainability

358 Note that in this study we only considered chemical feature-based models, while recently we
359 observed many deep learning models now directly analyse chemical structure such as SMILE
360 string, InChI key, 3D image as the model input^{49, 50}. Directly using chemical structure instead
361 of features may be a game changer to the predictive toxicology, just like the current image
362 analysis nowadays will directly use the raw image rather than human-engineered features.
363 The investigation and comparison between feature-based and feature-free models also need to
364 be comprehensively performed. In addition, consensus modeling could also be an effective
365 way to improve model predictivity⁵¹. Evaluation the explainability of consensus model is also
366 a challenge and the objective of future studies. While we plan to perform such studies
367 ourselves we also encourage the other researchers to analyze the data of this study, which
368 contain nearly 440k measurements for 65 properties (Supplementary table S2) in order to
369 propose and benchmark approaches balancing predictivity and explainability of models.

370 Future directions can also include evaluating metrics to qualitatively or quantitatively
371 measure the interpretability on demand, in order to investigate how much interpretability
372 could be gained by using different approaches and whether they contribute the same
373 interpretations. In addition, multi-task learning was proved to be an efficient way to improve
374 the model performance by sharing the modeling architectures among different predictive
375 endpoints^{14, 17, 19}. We also observed the same tendency in this study but a more
376 comprehensive investigation on the effects of multi-task learning compared to single-task
377 learning would be critical to better elucidate impact of these methods on the predictive
378 toxicology.

379 Acknowledgements

380 This research was supported in part by the Intramural/Extramural research program of the
381 NCATS, NIH and by the China Scholarship Council (CSC) for ZX (201706880010). The
382 authors thank Joanne Berger, FDA Library, for manuscript editing assistance.

383
384

385 Supporting Information

386 **Table S1.** Averaged training and testing AUC for 65 Tox21 assays

387 **Table S2.** Processed dataset of the Chemicals and Tox21 Endpoints used in this study

388

389 References

- 390 (1) Krizhevsky, A., Sutskever, I., and Hinton, G. E. (2012) Imagenet classification with deep convolutional
391 neural networks, In *Advances in neural information processing systems* pp 1097-1105.
- 392 (2) Chen, M., Borlak, J., and Tong, W. (2013) High lipophilicity and high daily dose of oral medications are
393 associated with significant risk for drug - induced liver injury. *Hepatology* 58, 388-396.
- 394 (3) Chen, M., Borlak, J., and Tong, W. (2016) A Model to predict severity of drug - induced liver injury in
395 humans. *Hepatology* 64, 931-940.
- 396 (4) Wu, L., Liu, Z., Auerbach, S., Huang, R., Chen, M., McEuen, K., Xu, J., Fang, H., and Tong, W. (2017)
397 Integrating Drug's Mode of Action into Quantitative Structure–Activity Relationships for Improved
398 Prediction of Drug-Induced Liver Injury. *Journal of chemical information and modeling* 57, 1000-1006.
- 399 (5) Hong, H., Thakkar, S., Chen, M., and Tong, W. (2017) Development of decision forest models for
400 prediction of drug-induced liver injury in humans using a large set of FDA-approved drugs. *Scientific*
401 *reports* 7, 1-15.
- 402 (6) Khadka, K. K., Chen, M., Liu, Z., Tong, W., and Wang, D. (2020) Integrating adverse outcome pathways
403 (AOPs) and high throughput in vitro assays for better risk evaluations, a study with drug-induced liver
404 injury (DILI). *ALTEX-Alternatives to animal experimentation* 37, 187-196.
- 405 (7) Tong, W., Cao, X., Harris, S., Sun, H., Fang, H., Fuscoe, J., Harris, A., Hong, H., Xie, Q., and Perkins, R.
406 (2003) ArrayTrack--supporting toxicogenomic research at the US Food and Drug Administration
407 National Center for Toxicological Research. *Environmental health perspectives* 111, 1819-1826.
- 408 (8) Bushel, P. R., and Tong, W. (2018) Integrative Toxicogenomics: Analytical Strategies to Amalgamate
409 Exposure Effects With Genomic Sciences. *Frontiers in genetics* 9, 563.
- 410 (9) Liu, Z., Huang, R., Roberts, R., and Tong, W. (2019) Toxicogenomics: a 2020 vision. *Trends in*
411 *Pharmacological Sciences* 40, 92-103.
- 412 (10) Huang, R., Xia, M., Sakamuru, S., Zhao, J., Shahane, S. A., Attene-Ramos, M., Zhao, T., Austin, C. P.,
413 and Simeonov, A. (2016) Modelling the Tox21 10 K chemical profiles for in vivo toxicity prediction and
414 mechanism characterization. *Nature communications* 7, 1-10.
- 415 (11) Luechtefeld, T., Marsh, D., Rowlands, C., and Hartung, T. (2018) Machine learning of toxicological big
416 data enables read-across structure activity relationships (RASAR) outperforming animal test
417 reproducibility. *Toxicological Sciences* 165, 198-212.
- 418 (12) Thakkar, S., Li, T., Liu, Z., Wu, L., Roberts, R., and Tong, W. (2020) Drug-induced liver injury severity
419 and toxicity (DILIst): Binary classification of 1279 drugs by human hepatotoxicity. *Drug discovery today*
420 25, 201-208.

- 421 (13) Richard, A. M., Huang, R., Waidyanatha, S., Shinn, P., Collins, B. J., Thillainadarajah, I., Grulke, C. M.,
422 Williams, A. J., Lougee, R. R., and Judson, R. S. (2020) The Tox21 10K Compound Library: Collaborative
423 Chemistry Advancing Toxicology. *Chemical Research in Toxicology*.
- 424 (14) Mayr, A., Klambauer, G., Unterthiner, T., and Hochreiter, S. (2016) DeepTox: toxicity prediction using
425 deep learning. *Frontiers in Environmental Science* 3, 80.
- 426 (15) Ghasemi, F., Mehridehnavi, A., Perez-Garrido, A., and Perez-Sanchez, H. (2018) Neural network and
427 deep-learning algorithms used in QSAR studies: merits and drawbacks. *Drug Discov. Today* 23, 1784-
428 1790.
- 429 (16) Ghasemi, F., Mehridehnavi, A., Fassihi, A., and Pérez-Sánchez, H. (2018) Deep neural network in QSAR
430 studies using deep belief network. *Applied Soft Computing* 62, 251-258.
- 431 (17) Zakharov, A. V., Zhao, T., Nguyen, D.-T., Peryea, T., Sheils, T., Yasgar, A., Huang, R., Southall, N., and
432 Simeonov, A. (2019) Novel consensus architecture to improve performance of large-scale multitask
433 deep learning QSAR models. *Journal of Chemical Information and Modeling* 59, 4613-4624.
- 434 (18) Chakravarti, S. K., and Alla, S. R. M. (2019) Descriptor free QSAR modeling using deep learning with
435 long short-term memory neural networks. *Frontiers in Artificial Intelligence* 2, 17.
- 436 (19) Sosnin, S., Karlov, D., Tetko, I. V., and Fedorov, M. V. (2018) Comparative study of multitask toxicity
437 modeling on a broad chemical space. *Journal of chemical information and modeling* 59, 1062-1072.
- 438 (20) LeCun, Y., Bengio, Y., and Hinton, G. (2015) Deep learning. *nature* 521, 436-444.
- 439 (21) Chen, H., Engkvist, O., Wang, Y., Olivecrona, M., and Blaschke, T. (2018) The rise of deep learning in
440 drug discovery. *Drug discovery today* 23, 1241-1250.
- 441 (22) Tetko, I. V., and Engkvist, O. (2020) From Big Data to Artificial Intelligence: chemoinformatics meets
442 new challenges. *Journal of Cheminformatics*.
- 443 (23) Samek, W., Montavon, G., Vedaldi, A., Hansen, L. K., and Müller, K.-R. (2019) *Explainable AI:*
444 *interpreting, explaining and visualizing deep learning*. Vol. 11700, Springer Nature.
- 445 (24) Arrieta, A. B., Díaz-Rodríguez, N., Del Ser, J., Bennetot, A., Tabik, S., Barbado, A., García, S., Gil-López,
446 S., Molina, D., and Benjamins, R. (2020) Explainable Artificial Intelligence (XAI): Concepts, taxonomies,
447 opportunities and challenges toward responsible AI. *Information Fusion* 58, 82-115.
- 448 (25) Jiménez-Luna, J., Grisoni, F., and Schneider, G. (2020) Drug discovery with explainable artificial
449 intelligence. *Nature Machine Intelligence* 2, 573-584.
- 450 (26) Huang, R., Xia, M., Sakamuru, S., Zhao, J., Shahane, S. A., Attene-Ramos, M., Zhao, T., Austin, C. P.,
451 and Simeonov, A. (2016) Modelling the Tox21 10 K chemical profiles for in vivo toxicity prediction and
452 mechanism characterization. *Nat Commun* 7, 10425.
- 453 (27) Tox21. (2017) Tox21 assays.
- 454 (28) Huang, R. (2016) A Quantitative High-Throughput Screening Data Analysis Pipeline for Activity
455 Profiling, In *High-Throughput Screening Assays in Toxicology* (Zhu, H., and Xia, M., Eds.), Humana
456 Press.
- 457 (29) Tetko, I. V. (2008) Associative neural network, In *Artificial Neural Networks* pp 180-197, Springer.
- 458 (30) Chen, T., and Guestrin, C. (2016) Xgboost: A scalable tree boosting system, In *Proceedings of the 22nd*
459 *acm sigkdd international conference on knowledge discovery and data mining* pp 785-794.
- 460 (31) Chang, C.-C., and Lin, C.-J. (2011) LIBSVM: A library for support vector machines. *ACM transactions on*
461 *intelligent systems and technology (TIST)* 2, 1-27.
- 462 (32) Pedregosa, F., Varoquaux, G., Gramfort, A., Michel, V., Thirion, B., Grisel, O., Blondel, M., Prettenhofer,
463 P., Weiss, R., and Dubourg, V. (2011) Scikit-learn: Machine learning in Python. *the Journal of machine*
464 *Learning research* 12, 2825-2830.
- 465 (33) Suykens, J. A., and Vandewalle, J. (1999) Least squares support vector machine classifiers. *Neural*
466 *processing letters* 9, 293-300.
- 467 (34) Breiman, L. (1996) Bagging predictors. *Machine learning* 24, 123-140.
- 468 (35) Baskin, I. I., Winkler, D., and Tetko, I. V. (2016) A renaissance of neural networks in drug discovery.
469 *Expert opinion on drug discovery* 11, 785-795.
- 470 (36) Sushko, I., Novotarskyi, S., Körner, R., Pandey, A. K., Rupp, M., Teetz, W., Brandmaier, S., Abdelaziz, A.,
471 Prokopenko, V. V., and Tanchuk, V. Y. (2011) Online chemical modeling environment (OCHEM): web
472 platform for data storage, model development and publishing of chemical information. *Journal of*
473 *computer-aided molecular design* 25, 533-554.
- 474 (37) (2020) The RDKit Book (https://www.rdkit.org/docs/RDKit_Book.html, access on 11/22/2020).
- 475 (38) Salmina, E. S., Haider, N., and Tetko, I. V. (2016) Extended functional groups (EFG): an efficient set for
476 chemical characterization and structure-activity relationship studies of chemical compounds.
477 *Molecules* 21, 1.

- 478 (39) Yang, C., Tarkhov, A., Maruszczyk, J. r., Bienfait, B., Gasteiger, J., Kleinoeder, T., Magdziarz, T., Sacher,
479 O., Schwab, C. H., and Schwoebel, J. (2015) New publicly available chemical query language, CSRML,
480 to support chemotype representations for application to data mining and modeling. *Journal of*
481 *Chemical Information and Modeling* 55, 510-528.
- 482 (40) Moriwaki, H., Tian, Y.-S., Kawashita, N., and Takagi, T. (2018) Mordred: a molecular descriptor
483 calculator. *Journal of cheminformatics* 10, 4.
- 484 (41) Hong, H., Xie, Q., Ge, W., Qian, F., Fang, H., Shi, L., Su, Z., Perkins, R., and Tong, W. (2008) Mold2,
485 molecular descriptors from 2D structures for chemoinformatics and toxicoinformatics. *Journal of*
486 *chemical information and modeling* 48, 1337-1344.
- 487 (42) Haider, N. (2010) Functionality pattern matching as an efficient complementary structure/reaction
488 search tool: an open-source approach. *Molecules* 15, 5079-5092.
- 489 (43) Scikit-Learn. (2020) SVC (<https://scikit-learn.org/stable/modules/generated/sklearn.svm.SVC.html>,
490 access on 11/22/2020).
- 491 (44) Consortium, M. (2010) The MicroArray Quality Control (MAQC)-II study of common practices for the
492 development and validation of microarray-based predictive models. *Nature biotechnology* 28, 827.
- 493 (45) Ribeiro, M. T., Singh, S., and Guestrin, C. (2016) Model-agnostic interpretability of machine learning.
494 *arXiv preprint arXiv:1606.05386*.
- 495 (46) Ribeiro, M. T., Singh, S., and Guestrin, C. (2016) " Why should i trust you?" Explaining the predictions
496 of any classifier, In *Proceedings of the 22nd ACM SIGKDD international conference on knowledge*
497 *discovery and data mining* pp 1135-1144.
- 498 (47) Zafar, M. R., and Khan, N. M. (2019) DLIME: A deterministic local interpretable model-agnostic
499 explanations approach for computer-aided diagnosis systems. *arXiv preprint arXiv:1906.10263*.
- 500 (48) Finn, C., Abbeel, P., and Levine, S. (2017) Model-agnostic meta-learning for fast adaptation of deep
501 networks. *arXiv preprint arXiv:1703.03400*.
- 502 (49) Karpov, P., Godin, G., and Tetko, I. V. (2019) Transformer-CNN: Fast and Reliable tool for QSAR. *arXiv*
503 *preprint arXiv:1911.06603*.
- 504 (50) Sosnin, S., Vashurina, M., Withnall, M., Karpov, P., Fedorov, M., and Tetko, I. V. (2019) A survey of
505 multi - task learning methods in chemoinformatics. *Molecular informatics* 38, 1800108.
- 506 (51) Novotarskyi, S., Abdelaziz, A., Sushko, Y., Körner, R., Vogt, J., and Tetko, I. V. (2016) ToxCast EPA in
507 vitro to in vivo challenge: insight into the Rank-I model. *Chemical research in toxicology* 29, 768-775.

508